# Surface restructuring under gas pressure from first principles: A mechanism for CO-induced removal of the Au(110)-(1×2) reconstruction

D. Loffreda,[1,*] L. Piccolo,[2] and P. Sautet[1]
[1]*Laboratoire de Chimie, UMR CNRS 5182, Ecole Normale Supérieure de Lyon, 46 Allée d'Italie, F-69364 Lyon Cedex 07, France*
[2]*Institut de Recherches sur la Catalyse, UPR CNRS 5401, 2 Avenue Albert Einstein, F-69626 Villeurbanne Cedex, France*
(Received 16 November 2004; published 30 March 2005)

Through an interplay between atomistic thermodynamics, isotherm models, and kinetics, all based on density functional theory calculations, we propose a mechanism for the removal of the $(1\times2)$ missing-row reconstruction on Au(110) under high CO pressure. Elevating the pressure from ultrahigh vacuum to one atmosphere causes the emergence of adsorption structures containing Au-CO entities. It is argued that the formation and the diffusion of these species may be the general phenomena which may control the morphology of metal surfaces under elevated CO pressure.

DOI: 10.1103/PhysRevB.71.113414 PACS number(s): 68.43.Bc, 68.35.Md, 68.43.Jk

Many of the present-day first-principles approaches of heterogeneous catalysis mechanisms are achieved by considering the metallic substrate as a static support and by neglecting the surrounding environment. However, the incidence of a high pressure of reactants and a high temperature on the surface morphology and on the catalyst performance calls into question this simplified model.[1–5] In this Brief Report we show how a high reactant pressure at room temperature (RT) can stabilize adsorbate overlayers which are not present in ultrahigh vacuum (UHV), and alter the surface structure of the catalyst. Moreover, a mechanism explaining the adsorption-induced removal of a missing-row reconstruction is proposed from density functional theory (DFT) calculations. We suggest the formation and the diffusion of carbonyl species to be the general phenomena which may change the morphology of metallic surfaces under elevated CO pressure.

The system chosen for illustration is CO/Au(110). Contrary to Pt(110),[6,7] an elevated CO pressure is necessary for removing the Au(110)-$(1\times2)$ missing-row reconstruction at RT.[4] In the latter case, a deep reorganization of the substrate, with the formation of steps, is observed by scanning tunneling microscopy (STM).

*Ab initio* theory connecting first-principles calculations with thermodynamics opens new horizons for theoretical studies of catalytic processes.[8] In this Brief Report we use atomistic thermodynamics and develop isotherm models and kinetics, all on the basis of DFT calculations, to show that a high CO pressure can remove the Au(110)-$(1\times2)$ reconstruction. The restructuring mechanism is initiated by an easy formation of Au-CO clusters due to the stabilization of Au single adatoms on the surface by CO adsorption. These carbonyl species, which diffuse along the missing rows, hence fill the empty troughs and lead to the unreconstructed surface.

DFT energies are calculated at the generalized gradient approximation (GGA) with the VASP program.[9,10] Various surfaces [$(1\times1)$, $(1\times2)$ reconstructed, steps, and adatoms] and adsorption structures are considered, as shown in Figs. 1 and 2.[13] For a given surface $i$ with an unit cell area $A_i$ containing $N_{CO}$ CO molecules, the coverage $\theta$ (%) is defined as the molecule density normalized to the smallest unit cell area $A_{1\times1}$ of Au(110)-$(1\times1)$: $\theta=100\times N_{CO}/A_i\times A_{1\times1}$.[14] Adsorption on steps is considered with the Au$(2\bar{3}0)$ vicinal surface $(2[110]\times[100])$. From the present calculations, the most favorable chemisorption site is always atop a Au atom.

Once the adsorption state is known from DFT calculations, its thermodynamic stability is given by the surface free energy $\gamma_{surf}$ per unit cell area $A$, which results from a balance between the energetic loss due to formation of the surface from the bulk and the gain due to adsorption. $\gamma_{surf}$ is calculated as the difference between the total Gibbs free energy of the chemisorbed system $G_{tot}$ and the chemical potentials of the Au bulk $\mu_{Au}^{bulk}$ and the gas phase $\mu_{CO}^{gas}$ references, as $\gamma_{surf}^{\theta}=(1/A)(G_{tot}^{\theta}-N_{Au}\mu_{Au}^{bulk}-N_{CO}\mu_{CO}^{gas})$, $N_{Au}$ and $N_{CO}$ being the total numbers of Au atoms and CO molecules present in the superstructure.[15–17] In the model, the CO gas phase plays the role of a reservoir which imposes its temperature $T$ and pressure $P$ to the adsorbed phase. In principle, the vibrational energy and entropy contributions to the Gibbs free energy should be considered. However, since the weak CO adsorption does not modify significantly the adsorbate vibrations and substrate phonons, these contributions can be neglected.[18] Hence, $G_{tot}^{\theta}$ and $\mu_{Au}^{bulk}$ are approximated as DFT total energies ($E_{tot}^{\theta}$ and $E_{Au}^{bulk}$, respectively). Within these simplifications, the surface free energy $\gamma_{surf}^{\theta}(T,P)$ reads

$$\gamma_{surf}^{\theta}(T,P)\approx\frac{1}{A}\left(E_{tot}^{\theta}-N_{Au}E_{Au}^{bulk}-N_{CO}E_{CO}^{gas}-N_{CO}kT\ln\left(\frac{1}{Z_{CO}^{t}(T,P)Z_{CO}^{r}(T)}\right)-N_{CO}kT\ln\left(\frac{P}{P_0}\right)\right),\quad(1)$$

where $Z_{CO}^{t}$ and $Z_{CO}^{r}$ are the translational and rotational partition functions of the gas phase (ln means logarithm to base $e$). To ensure a tight convergence of $\gamma_{surf}$ ($\leqslant1$ meV Å$^{-2}$), highly dense $k$-point meshes are used in the calculations. This numeric error is smaller than the systematic error due to

 ©2005 The American Physical Society

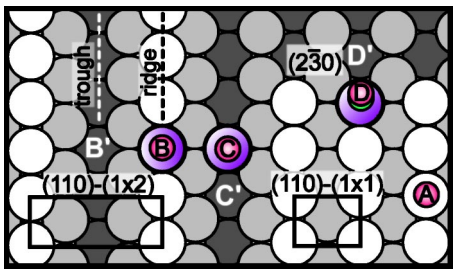


FIG. 1. (Color online) Top views of CO adsorption on: (A) bulk-terminated Au(110)-(1×1), (B) missing-row Au(110)-(1×2), (C) a Au adatom located in the troughs of Au-(1×2), and (D) a step of Au(2$\bar{3}$0). (B–B′) defines an extraction pathway of a Au-CO cluster from a ridge of Au(110)-(1×2), (C-C′) a diffusion pathway for a Au-CO cluster along a trough of Au(110)-(1×2), and (D-D′) an extraction pathway for a Au—CO cluster on Au(2$\bar{3}$0). The Au atoms of carbonyl clusters appear with shaded balls.

the basis set and the supercell approach (±5 meV Å$^{-2}$), as shown previously.[17,18]

In Fig. 3(a), the surface free-energy curves are plotted at 300 K as a function of the CO pressure for each considered structure and coverage. Without CO adsorption (UHV), the missing-row Au(110)-(1×2) surface has the lowest surface energy [cf. horizontal lines in Fig. 3(a)]. In the low-pressure regime (below 25 Torr, cf. area I), two superstructures on Au(110)-(1×2) show a similar high stability with a CO coverage of 16.67%: a (3×2) structure where CO adsorbs on a ridge and the same structure with CO adsorbed on a Au adatom positioned in a trough. Hence the energy cost to generatea Au adatom is compensated by the enhanced CO adsorption energy at this low coordination site compared to the ridge site. With respect to the bare surface, the adsorption structure on the ridges becomes thermodynamically stable for a pressure above 3 Torr. However, for lower pressures, adsorption can be initiated at defect sites ($10^{-1}$ Torr for adatoms).

Between 25 and $4\times10^3$ Torr (cf. area II), the structures involving Au adatoms clearly become the most stable ones

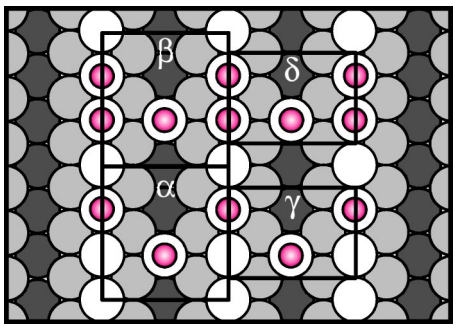


FIG. 2. (Color online) Top views of high coverage adsorption structures on Au-(1×2) presenting adatoms in the troughs of the missing rows. CO adsorbs on the adatoms and on the ridges with various coverages: ($\alpha$) (3×2)-2 CO (33.33%), ($\beta$) (3×2)-3 CO (50%), ($\gamma$) (2×2)-2 CO (50%), and ($\delta$) (2×2)-3 CO (75%). The superstructures refer to the (1×1) surface.

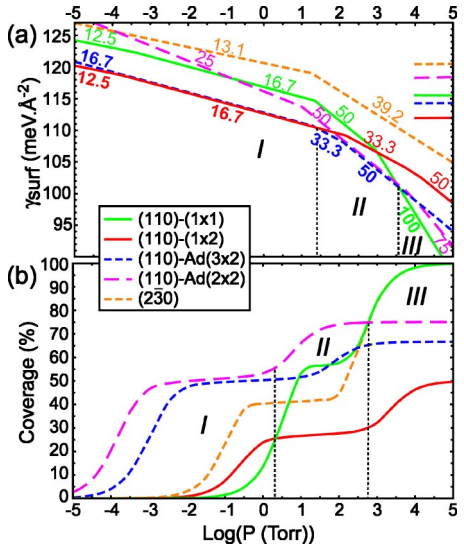


FIG. 3. (Color online) (a) Surface free-energy diagram (meV Å$^{-2}$) at 300 K as a function of the CO pressure P (Torr) for the various Au surfaces (log means logarithm to base 10). For each surface, the evolution of the CO coverage (%) is reported. The horizontal lines indicate the calculated surface energy of the bare metallic surfaces. (b) CO adsorption isotherms at 300 K for the various Au surfaces.

with a small influence of the superstructure of adatoms [(3×2) or (2×2)]. The CO coverage increases to 33.33% (structure $\alpha$) and then to 50% (structures $\beta$ and $\gamma$). Hence, in the 100 Torr range, CO adsorption allows to generate Au adatoms on the (1×2) surface.

In the high-pressure regime (above $4\times10^3$ Torr cf. area III), the (1×1) surface at saturation (100%) becomes the most stable one. This surface is indeed the only one which can favorably accommodate such a high CO density.

Contrary to the surface free-energy diagram, the evolution of the CO coverage with the pressure can be described continuously with the adsorption isotherms, which are measurable by the experimentalists. The isotherm model developed here is based on DFT adsorption energies $E_{ads}$ for a finite set of structures and coverages (cf. Fig. 4). $E_{ads}$ decreases with the coverage, in agreement with experiments.[19] The adsorption is weaker on the (1×1) and (1×2) surfaces than on the steps and on the adatoms. These results agree qualitatively with recent thermal desorption spectroscopy observations on

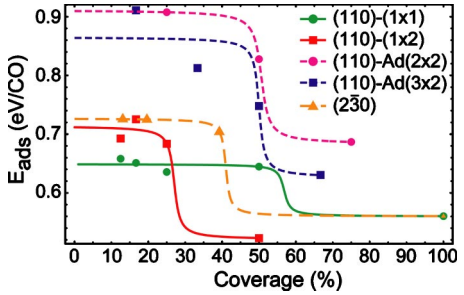


FIG. 4. (Color online) Adsorption energy (eV/CO molecule) as a function of CO coverage (%) over the various Au surfaces. The continuous lines correspond to arctan fits [cf. Eq. (2)].

TABLE I. Activation energies $E_{act}$ (eV) and diffusion coefficients $D_{300}$ ($cm^2\ s^{-1}$) calculated at 300 K for extraction (extr) and diffusion (diff) pathways of Au adatoms and Au-CO clusters (cf. B-B′, C-C′, and D-D′ in Fig. 1).

| Au | Structure ($\theta$ %) | $E_{act}^{extr}$ | $D_{300}^{extr}$ | $E_{act}^{diff}$ | $D_{300}^{diff}$ |
|---|---|---|---|---|---|
| (110) | (3×2)Ad (0) | 1.28 | $1\times10^{-24}$ | 0.50 | $5\times10^{-12}$ |
| | (3×2)Ad-1CO (16.7) | 0.85 | $2\times10^{-17}$ | 0.47 | $2\times10^{-11}$ |
| | (3×2)Ad-2CO (33.3) | | | 0.46 | $3\times10^{-11}$ |
| | (3×2)Ad-3CO (50.0) | | | 0.50 | $4\times10^{-12}$ |
| | (3×2)Ad-4CO (66.7) | | | 0.47 | $2\times10^{-11}$ |
| $(2\bar{3}0)$ | (3×1) (0) | 0.50 | $5\times10^{-12}$ | | |
| | (3×1)-1CO (13.08) | 0.44 | $7\times10^{-11}$ | | |

Au(110)-(1×2) (Ref. 20) where a lowering of the adsorption energy is reported from 0.61 eV (at zero coverage limit) to 0.36 eV (at 0.45 ML). A qualitative agreement is also obtained with Clausius-Clapeyron data analysis yielding a more moderate variation of the CO adsorption heat (from 0.47 to 0.34 eV).[19] In the isotherm model, $E_{ads}$ is fitted as a function of the coverage $\theta$ according to the following phenomenological model (cf. Fig. 4):

$$E_{ads}(\theta) = E_{1/2} + E_0 \arctan(\theta_{1/2} - x\theta). \quad (2)$$

This fit is inspired by IRAS (infrared reflection-absorption spectroscopy) measurements[19] showing that the adsorption energy is finite at zero coverage and nonzero at saturation. The model depends on three parameters, the adsorption energy for half a monolayer $E_{1/2}$, the energy amplitude $E_0$ and the parameter $x$, the coverage of half monolayer $\theta_{1/2}$ being fixed.

The adsorption isotherm of CO on Au surfaces is calculated at the equilibrium of the adsorption-desorption processes.[21] Moreover, the gas-phase translational and rotational partition functions ($\tilde{Z}_{CO}^{t}$ and $Z_{CO}^{r}$, respectively) are included in the model,

$$P = kT\tilde{Z}_{CO}^{t}(T)Z_{CO}^{r}(T)\frac{\theta}{\theta_{sat}-\theta}\exp\left(\frac{-E_{ads}(\theta)}{kT}\right), \quad (3)$$

where $\theta_{sat}$ is the saturation coverage. In this model, the choice of the GGA functional is important. The Perdew Wang 91 functional[11] provides the best agreement between calculated adsorption energies and recent desorption measurements.[20] However, the estimation of the pressure is semiquantitative since the error obtained for $E_{ads}$ (0.1 eV) leads to an uncertainty of 1–2 orders of magnitude in pressure.

In Fig. 3(b), the adsorption isotherms are plotted for all the Au surfaces at 300 K. Below 2 Torr (cf. area I), the CO coverage is higher on Au(110)-(1×2) than on Au(110)-(1×1), in the same pressure range. The isotherm model hence agrees with the surface free-energy diagram described previously. However, the coverage is maximal on the structures with Au adatoms [stable Ad-(3×2) and metastable Ad-(2×2)]. As a consequence, the surface should exhibit large domains with perfect missing rows, while some domains with adatoms would start to nucleate under CO pressure. Between 2 and 500 Torr (cf. area II), the coverage increases again for the adatom structures, both stable, and the restructuring of the surface is effective. At higher pressures (cf. area III), the coverage is maximum on the (1×1) surface. Since this is the most stable surface, the phase transition should be completed.

According to thermodynamics, the driving force for restructuring the missing-row Au(110) surface at 300 K is the unexpected stability of the adatom structures under elevated CO pressure. However, kinetics might hinder the deconstruction with high activation energy barriers for the formation of adatoms and their diffusion along the channels. In order to analyze this scenario, the extraction and diffusion pathways of Au atoms and Au-CO clusters have been studied with the climbing image nudged-elastic band method.[22] The activation energy is estimated with the minimization of eight intermediate images along the pathway. The results are reported in Table I. The extraction of a Au atom from a ridge of Au(110)-(1×2) is an endothermic process (0.55 eV) having a high activation energy (1.28 eV). The adsorption of CO on the Au atom to be extracted (cf. B–B′ in Fig. 1) greatly reduces the endothermicity (0.30 eV) and the activation barrier (0.85 eV). Hence the formation of an adatom is strongly facilitated by chemisorption. The diffusion coefficient $D_{300}^{extr}$ calculated with the transition-state theory (TST) (Ref. 23) is thus large ($2\times10^{-17}\ cm^2\ s^{-1}$).[24] The extraction of Au atoms is even easier from the steps of Au$(2\bar{3}0)$. Without CO, the activation energy is already low (0.50 eV), leading to a high diffusivity ($5\times10^{-12}\ cm^2\ s^{-1}$). However, the extraction of a Au-CO cluster is favored again (0.44 eV, cf. D–D′ in Fig. 1). Hence the adsorption of CO activates preferentially the formation of Au-CO clusters not only from the ridges of the missing-row reconstructed surface but also from the steps, where extraction kinetics are clearly favored.

Once the adatoms are formed, their diffusion requires an activation energy of 0.50 eV in the absence of CO, which is slightly higher than the one measured by low-temperature STM (0.40–0.44 eV).[26] However, GGA calculations provide a slightly better agreement with experiments than previous semiempirical RGL (Rosato, Guillopè, and Legrand) potentials (0.31 eV).[27] When CO is adsorbed on Au adatoms

(cf. C−C′ in Fig. 1), the activation energy is similar (0.46−0.5 eV) for a large range of coverage (from 16.7% to 66.7%). As a result, the diffusion of Au—CO clusters and Au adatoms is not limited kinetically. Kinetics thus support the scenario suggested from thermodynamics.

In conclusion, the mechanism of a surface restructuring under a gas pressure can be understood from kinetics and thermodynamics connected with first-principles calculations. According to our models, a high CO pressure (between 10 and 100 Torr) removes the $(1\times2)$ missing-row reconstruction on Au(110). The proposed scenario is the following. High-pressure CO adsorption along the ridges or the steps would allow the formation of Au-CO clusters. These species, which diffuse easily along the empty troughs, would finally fill the missing rows and would generate the unreconstructed Au(110)-$(1\times1)$ surface. The existence of carbonyl clusters has been mentioned previously on Pt(110)-$(1\times2)$ from high-pressure STM experiments.[5] Our results support the argument of an ability for CO to create its own low-coordinated adsorption sites and remove the $(1\times2)$ reconstruction. An experimental validation of our scenario would require especially room-temperature STM observations with atomic resolution above one atmosphere of CO, in order to reach the $(1\times1)$ structure completion over the terraces.

More generally, the stabilization of adsorption structures containing carbonyl species under a high gas pressure suggests that model approaches of heterogeneous catalysis should include the temperature and pressure effects, for improving our knowledge of realistic catalytic systems.

The authors acknowledge IDRIS at Orsay (France) for CPU time and assistance.

*Electronic address: David.Loffreda@ens-lyon.fr

[1] B. J. McIntyre, M. Salmeron, and G. A. Somorjai, J. Vac. Sci. Technol. A **11**, 1964 (1993).
[2] K. F. Peters, P. Steadman, H. Isern, J. Alvarez, and S. Ferrer, Surf. Sci. **467**, 10 (2000).
[3] B. L. M. Hendriksen and J. W. M. Frenken, Phys. Rev. Lett. **89**, 046101 (2002).
[4] Y. Jugnet, F. J. Cadete Santos Aires, C. Deranlot, L. Piccolo, and J. C. Bertolini, Surf. Sci. **521**, L639 (2002).
[5] P. Thostrup, P. K. Vertergaard, T. An, E. Laegsgaard, and F. Besenbacher, J. Chem. Phys. **118**, 3724 (2003).
[6] T. Gritsch, D. Coulman, R. J. Behm, and G. Ertl, Phys. Rev. Lett. **63**, 1086 (1989).
[7] P. Thostrup, E. Christoffersen, H. T. Lorensen, K. W. Jacobsen, F. Besenbacher, and J. K. Nørskov, Phys. Rev. Lett. **87**, 126102 (2001).
[8] K. Reuter and M. Scheffler, Phys. Rev. Lett. **90**, 046103 (2003).
[9] G. Kresse and J. Furthmüller, Phys. Rev. B **54**, 11 169 (1996).
[10] We use the Perdew Wang 91 exchange-correlation functional (Ref. 11) and the PAW method (Ref. 12). The plane-wave cutoff is set to 400 eV.
[11] J. Perdew and Y. Wang, Phys. Rev. B **45**, 13 244 (1992).
[12] G. Kresse and D. Joubert, Phys. Rev. B **59**, 1758 (1999).
[13] The adsorption of CO molecules on Au surfaces is modeled with nonsymmetrized six-layer-thick slabs.
[14] Adstructures and coverages referring to Au(110)-$(1\times1)$: $(1\times1)$ 100%, $(2\times1)$, $(1\times2)$ or $c(2\times2)$ 50%, $(2\times2)$ 25%, $(3\times2)$ 16.67%, $(4\times2)$ 12.5%, for Au(110)-$(1\times1)$; $(1\times2)$ 50%, $(3\times2)$ 33.33%, $(2\times2)$ 25%, $(3\times2)$ 16.67%, $(4\times2)$ 12.5%, for Au(110)-$(1\times2)$; $(1\times1)$ 39.25%, $(2\times1)$ 19.63%, $(3\times1)$ 13.08%, for Au($2\bar{3}0$), varying the coverage along the steps, where the adsorption is preferential.
[15] E. Kaxiras, Y. Bar-Yam, J. D. Joannopoulos, and K. C. Pandey, Phys. Rev. B **35**, 9625 (1987).
[16] G.-X. Qian, R. M. Martin, and D. J. Chadi, Phys. Rev. B **38**, 7649 (1988).
[17] K. Reuter and M. Scheffler, Phys. Rev. B **68**, 045407 (2003).
[18] K. Reuter and M. Scheffler, Phys. Rev. B **65**, 035406 (2001).
[19] D. C. Meier, V. Bukhtiyarov, and D. W. Goodman, J. Phys. Chem. B **107**, 12668 (2003).
[20] J. M. Gottfried, J. J. Schmidt, S. L. M. Schroeder, and K. Christmann, Surf. Sci. **536**, 206 (2003).
[21] J. A. W. Elliott and C. A. Ward, Langmuir **13**, 951 (1997).
[22] G. Henkelman, B. P. Uberuaga, and H. Jonsson, J. Chem. Phys. **113**, 9901 (2000).
[23] R. A. van Santen and J. W. Niemantsverdriet, *Chemical Kinetics and Catalysis* (Plenum, New York, 1995).
[24] The calculated preexponential factor $D_0$ ($2\times10^{-3}$ cm$^2$ s$^{-1}$) agrees with previous Monte Carlo Variational TST results ($0.80\times10^{-4}-0.40\times10^{-1}$ cm$^2$ s$^{-1}$) (Ref. 25).
[25] P. M. Agrawal, B. M. Rice, and D. L. Thompson, Surf. Sci. **515**, 21 (2002).
[26] S. Gunther, A. Hittzke, and R. J. Behm, Surf. Rev. Lett. **4**, 1103 (1997).
[27] F. Montalenti and R. Ferrando, Phys. Rev. B **59**, 5881 (1999).